Physical Communication 24 (2017) 182–194

Contents lists available at ScienceDirect

Physical Communication

journal homepage: www.elsevier.com/locate/phycom

Full length article

Spectrum sensing for OFDM signals using pilot induced cyclostationarity in the presence of cyclic frequency offset

Ribhu Chopra *,[1], Debashis Ghosh, D.K. Mehra

Department of Electronics and Communication Engineering, Indian Institute of Technology Roorkee, Uttarakhand, India

ARTICLE INFO

Article history:
Received 10 April 2016
Received in revised form 9 May 2017
Accepted 24 July 2017
Available online 1 August 2017

Keywords:
Cognitive radio
Spectrum sensing
Cyclostationarity
OFDM spectrum sensing
Cyclic frequency offset

ABSTRACT

In this paper, the problem of spectrum sensing of OFDM signals for cognitive radios is considered. It is proposed to detect the cyclostationary features introduced in an OFDM signal due to inter-pilot correlation. The performance of the proposed detector is derived and verified in case of AWGN channels. It is observed that the performance of cyclostationary detectors relies on the knowledge of the exact value of the cyclic frequency of the signal of interest. However, an offset in the cyclic frequency may arise due to several reasons. Therefore, for the proposed detector to perform reliably, there is a need to estimate the cyclic frequency offset. The Cramer–Rao bound for the cyclic frequency offset (CFO) estimator is derived, and based on it, two algorithms to estimate and compensate for the CFO are proposed. Simulation results are then used to study the performance of the proposed detection technique under Rayleigh fading both in the presence and the absence of CFO. The performance of the proposed system model is also studied under fast fading, and an alternative test statistic is proposed.

1. Introduction

During the past few years, the opportunistic spectrum access (OSA) model has received much attention due to its ability to combat the dual problems of spectrum shortage and under-utilization. Under this model, unlicensed secondary users opportunistically access unused portions of the licensed spectrum. In accordance with this model, cognitive radios sense the spectrum for vacancies and utilize them accordingly [1]. It must, however, be noted that the primary users sharing their spectrum are predominantly legacy systems such as digital television and wireless microphones, which have a user base as well as an infrastructure in place. It is therefore necessary that this infrastructure remains unaffected when OSA is implemented. In other words, the cognitive radio system accessing the spectrum opportunistically must be transparent to the primary users. Hence, it is necessary for the cognitive radio to efficiently sense the spectrum and detect the presence of a primary user signal. For this purpose, it is essential that the sensitivity of a secondary user towards the primary signal should be more than the primary receiver [2].

The most popular approach for spectrum sensing is the energy detection approach that involves measuring power contained in the band of interest and then comparing it against the background noise power. Though this is the optimal detector for random signal detection [3], it requires the exact knowledge of the noise power. Otherwise, the energy detector fails to sense the spectrum due to the phenomenon of SNR walls [4]. As a result, it is desired that certain properties of the primary user signal, absent in the channel noise should be used to aid its detection. These properties may be the entire signal structure [5], the pilot information [6], or statistical properties of the primary signal [7].

OFDM (Orthogonal Frequency Division Multiplexing) is a popular wide band digital modulation technique because of its ease of implementation and flexibility. For OSA to be implemented in a network employing OFDM for modulation, it is necessary to develop techniques that can distinguish an OFDM signal from the background noise. Most of the methods developed for OFDM signal detection are based on the detection of one or more inherent features, such as the cyclic prefix or the pilot tones. In [8] the authors propose to use the autocorrelation properties introduced due to the cyclic prefix as features to detect the primary signal. The authors in [9] also use the cyclic prefix as a distinguishing feature in the OFDM system and have developed optimal and sub-optimal detectors to detect the non-stationarity caused due to the cyclic prefix. The cyclic autocorrelation function and the sign cyclic autocorrelation function have respectively been used to detect

* Corresponding author.
E-mail addresses: ribhu@outlook.com (R. Chopra), ghoshfec@iitr.ac.in (D. Ghosh), dkmecfec@iitr.ac.in (D.K. Mehra).
[1] Now at: Department of Electronics and Electrical Engineering, Indian Institute of Technology Guwahati, Assam, India.

http://dx.doi.org/10.1016/j.phycom.2017.07.008
1874-4907/

the cyclostationary features introduced due to the cyclic prefix in [10] and [11]. The authors in [12] use time domain symbol cross-correlation to detect the correlation introduced by the pilot tones. This property has also been exploited in [13] where finite time autocorrelation function is used as a test statistic. The authors in [14] use the empirical cyclic spectral density to detect cyclostationarity introduced due to correlated pilots. The difference in the statistical properties of the pilot and data subcarriers is exploited in [15] for primary signal detection. Artificially induced cyclostationary features to assist OFDM signal detection are proposed in [16] and have subsequently been used in [17].

The methods based on induced cyclostationarity require changing the primary user signal structure while those based on the cyclic prefix are weak and susceptible to change with channel conditions. In view of this, this paper proposes a detector which uses the cyclostationarity induced due to correlated pilot tones. The signal model considered here is similar to the one used in [14]. However, instead of using the cyclic spectral density at different frequencies, this paper proposes to use the cyclic autocorrelation function to sense the presence of OFDM signals. It may be observed that the multi-cycle autocorrelation based detector does not require symbol level synchronization at the spectrum sensor, which is an advantage over the approach used in [14].

It is observed that most communication signals exhibit cyclostationarity only for a set of discrete cyclic frequencies. The performance of a cyclostationarity detector, therefore is dependent on the correct knowledge of these frequencies. Unfortunately, it cannot be ensured that the cyclic frequency known at the cognitive radio terminal and the cyclic frequency of the primary signal are the same. An offset between the actual and the known values of the cyclic frequencies may arise if the channel causes a significant Doppler shift in the primary user signal, or if there is an offset in the sampling clock [14,18–20]. The effects of cyclic frequency offset (CFO) on the detection performance are severe as shown in [20]. The authors in [20], also propose a mechanism to bypass the effects of CFO by averaging the test statistics over smaller sample blocks. However, this technique causes a loss in the number of features being used for detection thereby compromising the detection performance. As an alternative, we propose in [21] to first estimate the CFO and then compensate for its effects so as to keep the number of features being used for detection unchanged. In [22], we use the CFO estimation technique proposed in [21] for estimating the true cyclic frequency of the adaptation stage of a FRESH filter based spectrum sensing. In this paper we extend the work of [21] and propose another approach based on gradient ascent for countering the effects of CFO in cyclostationarity based spectrum sensing. It is shown via simulation that these approaches offers a gain of nearly 6dB over the approach presented in [20], but at the cost of a higher computational complexity.

The detector for cyclostationary features introduced due to correlated pilots has been derived along with its performance in Section 2. The effect of CFO on the detector performance is derived and the necessity for CFO estimation is explained in Section 3. Section 4 derives the Cramer–Rao bound on the performance of a CFO estimator. Using this bound, Section 5 proposes a iterative CFO estimation algorithm based on gradient ascent while Section 6 proposes a higher complexity CFO estimation algorithm based on the greedy search approach. Simulation results are presented in Section 7 following which the conclusions are drawn in Section 9. We also consider the performance of the proposed system model under a fast fading channel, and propose an alternative test statistic in Section 8.

2. Signal model and the proposed detector

2.1. The primary user signal model

Let the primary user OFDM signal consist of N_d data sub-carriers. Out of these, let N_p be uniformly spaced pilot sub-carriers whose locations are given by the elements of the index set Π. Let the OFDM symbol use a cyclic prefix of length N_c resulting in a total OFDM symbol length $N = N_c + N_d$. If the symbol being sent over the mth sub-carrier of the kth OFDM symbol is given as $s_k[m]$ then, as in [14], the following two conditions are assumed to be satisfied. First, the magnitudes and phases of the pilots remain constant over all OFDM symbols, i.e. for $m \in \Pi$

$$s_k[m] = p[m] = \sqrt{\mathcal{E}_s} e^{j\theta_m} \quad \forall k \tag{1}$$

where $\mathcal{E}_s$ is the average subcarrier energy of the OFDM symbol and θ_m is the phase associated with the mth subcarrier. Secondly, it is assumed that correlation exists between the pilot values and is purely a function of the difference in pilot locations i.e. for $m, l \in \Pi$

$$p[m]p^*[l] = \mathcal{E}_s e^{j\theta_{m-l}}. \tag{2}$$

The primary signal transmitted at the nth instant of time may be written in the form

$$x[n] = \sum_k x_k[n - kN](u[n - kN] - u[n - (k+1)N]) \tag{3}$$

where, $u[n]$ is the discrete time unit step signal and $x_k[n]$ is the nth sample of the kth OFDM symbol, defined as

$$x_k[n] = \begin{cases} \dfrac{1}{\sqrt{N_d}} \displaystyle\sum_{m=1}^{N_d} s_k[m] e^{\frac{j2\pi mn}{N_d}} & 0 \le n \le N-1 \\ 0 & \text{otherwise.} \end{cases} \tag{4}$$

Now, for $0 \le n < N$ $x_k[n]$ may be re written as

$$\begin{aligned} x_k[n] &= \frac{1}{\sqrt{N_d}} \sum_{m=1}^{N_d} s_k[m] e^{\frac{j2\pi mn}{N_d}} \\ &= \frac{1}{\sqrt{N_d}} \sum_{m\in\Pi} s_k[m] e^{\frac{j2\pi mn}{N_d}} + \frac{1}{\sqrt{N_d}} \sum_{m\notin\Pi} s_k[m] e^{\frac{j2\pi mn}{N_d}} \\ &= \frac{1}{\sqrt{N_d}} \sum_{m\in\Pi} p[m] e^{\frac{j2\pi mn}{N_d}} + \frac{1}{\sqrt{N_d}} \sum_{m\notin\Pi} s_k[m] e^{\frac{j2\pi mn}{N_d}} \\ &= x_k^{(p)}[n] + x_k^{(d)}[n]. \end{aligned} \tag{5}$$

The pilot locations and values remain unchanged over different OFDM symbols. Therefore,

$$x_k^{(p)}[n] = x_m^{(p)}[n] \tag{6}$$

for the kth and mth OFDM symbols. Therefore,

$$x^{(p)}[n] = x^{(p)}[n + kN]. \tag{7}$$

That is, the contribution of the pilot terms remains unchanged over periodic shifts of the OFDM symbol.

2.2. The spectrum sensing model

The task of the spectrum sensor is to decide on the presence of a primary signal based on the received samples. It is assumed that the sensing receiver knows the transmitting signal parameters and the received signal is down-converted to baseband, while maintaining the sampling rate of the primary user. The received signal $y[n]$ under the two hypotheses may thus be written as

$$y[n] = \begin{cases} \nu[n] & \mathcal{H}_0 \\ x[n] + \nu[n] & \mathcal{H}_1 \end{cases} \tag{8}$$

where $\nu[n]$ is the zero mean complex Gaussian noise having a variance σ_ν^2, $\mathcal{H}_0$ is the null hypothesis corresponding to the absence of a primary signal and $\mathcal{H}_1$ is the alternate hypothesis corresponding to its presence.

Let $\hat{R}_{yy}^{\alpha}[M,\tau]$ be the finite time cyclic autocorrelation function at lag τ and frequency shift α, defined for M received samples as

$$\hat{R}_{yy}^{\alpha}[M,\tau]=\frac{1}{M-\tau}\sum_{n=\tau}^{M-1}y[n]y^{*}[n-\tau]e^{-j2\pi\alpha n}. \tag{9}$$

The signals $x[n]$ and $\nu[n]$ may both be assumed to be independent of each other. Also the individual samples of both $x[n]$ and $\nu[n]$ may be assumed as i.i.d. Gaussian [13,23,24]. Therefore, the samples of $y[n]$ may be assumed to be identically distributed Gaussian random variables. Further, using the central limit theorem, $\hat{R}_{yy}^{\alpha}[M,\tau]$ may be shown to have a Gaussian distribution [24]. Therefore, the performance of this detector can be determined by obtaining the moments of the test statistic under the two hypotheses as [21]

$$\hat{R}_{yy}^{\alpha}[M,\tau]\,|\mathcal{H}_0=\frac{1}{M-1}\sum_{n=\tau}^{M-\tau}\nu[n]\nu^{*}[n-\tau]e^{-j2\pi\alpha n}. \tag{10}$$

Now, since the noise is assumed to be zero mean wide sense stationary i.i.d.,

$$E\left[\hat{R}_{yy}^{\alpha}[M,\tau]\,|\mathcal{H}_0\right]=\sigma_\nu^2\delta(\alpha)\delta[\tau] \tag{11}$$

where $\delta(.)$ represents the Dirac Delta function, and $\delta[.]$ represents the Kronecker Delta function.

Similarly

$$\begin{aligned}\hat{R}_{yy}^{\alpha}[M,\tau]\,|\mathcal{H}_1=&\frac{1}{M-\tau}\sum_{n=\tau}^{M-1}(x^{(p)}[n]+x^{(d)}[n]+\nu[n])\\&\times(x^{(p)*}[n-\tau]+x^{(d)*}[n-\tau]+\nu^{*}[n-\tau])e^{-j2\pi\alpha n}.\end{aligned} \tag{12}$$

It may be noted that $x^{(d)}[n]$, $x^{(p)}[n]$ and $\nu[n]$ are zero mean and independent of each other as in [13,14]. Also it is important to note here that the contents of the data sub-carriers are assumed to be uncorrelated. Now,

$$\begin{aligned}E\left[\hat{R}_{yy}^{\alpha}[M,\tau]\,|\mathcal{H}_1\right]=&E\left[\frac{1}{M-\tau}\sum_{n=\tau}^{M-1}x^{(d)}[n]x^{*(d)}[n-\tau]e^{-j2\pi\alpha n}\right]\\&+E\left[\frac{1}{M-\tau}\sum_{n=\tau}^{M-1}x^{(p)}[n]x^{*(p)}[n-\tau]e^{-j2\pi\alpha n}\right]\\&+E\left[\frac{1}{M-\tau}\sum_{n=\tau}^{M-1}\nu[n]\nu^{*}[n-\tau]e^{-j2\pi\alpha n}\right].\end{aligned} \tag{13}$$

It may be shown that for a sufficiently large M

$$\begin{aligned}&\frac{1}{M-\tau}\sum_{n=\tau}^{M-1}x^{(p)}[n]x^{*(p)}[n-\tau]e^{-j2\pi\alpha n}\\&=\begin{cases}\dfrac{N_p}{N_d}\mathcal{E}_s e^{j\theta_\alpha} & \alpha=\dfrac{m-l}{N_d},\ m,l\in\Pi,\ \tau=kN\\ 0 & \text{otherwise}\end{cases}\end{aligned} \tag{14}$$

where θ_α is the phase of the cyclic autocorrelation function corresponding to the cyclic frequency α. For independent data symbols,

$$E\left[x^{(d)}[n]x^{*(d)}[n-\tau]e^{-j2\pi\alpha n}\right]=\begin{cases}\dfrac{N_c}{N}\mathcal{E}_s & \alpha=0,\ \tau=\pm N_d\\ \mathcal{E}_s & \alpha=0,\ \tau=0\\ 0 & \text{otherwise.}\end{cases} \tag{15}$$

The finite time cyclic autocorrelation function for $\alpha=\frac{m}{N_d}$, $m\in\{1,2,\ldots,N_p\}$ and $\tau=kN$, $k\in\{1,2,\ldots,\lfloor\frac{M}{N}\rfloor\}$ under the two hypotheses therefore becomes,

$$\hat{R}_{yy}[M,\tau]=\begin{cases}\xi_0[M,\tau] & \mathcal{H}_0\\ \dfrac{N_p}{N_d}\mathcal{E}_s e^{j\theta_\alpha}+\xi_1[M,\tau] & \mathcal{H}_1,\end{cases} \tag{16}$$

where, $\xi_0[M,\tau]$, $\xi_1[M,\tau]$ are the zero mean Gaussian distributed estimation errors arising due to finite time averaging of random signals. It may be shown that [3,13]

$$var\left(\xi_0[M,\tau]\right)=\frac{1}{M-\tau}\sigma_\nu^4 \tag{17}$$

$$var\left(\xi_1[M,\tau]\right)=\frac{1}{M-\tau}\left(\mathcal{E}_s+\sigma_\nu^2\right)^2. \tag{18}$$

Therefore, the distributions of $\hat{R}_{yy}^{\alpha}[M,\tau]$ for $\alpha=m\frac{1}{N_d}$, $m\in\{1,2,\ldots,N_p\}$ and $\tau=kN$, $k\in\left\{1,2,\ldots,\lfloor\frac{M}{N}\rfloor\right\}$ under the two hypotheses are

$$\hat{R}_{yy}^{\alpha}[M,\tau]\sim\begin{cases}\mathcal{N}_c\left(0,\dfrac{\sigma_\nu^4}{M-\tau}\right) & \mathcal{H}_0\\ \mathcal{N}_c\left(\dfrac{N_p}{N_d}\mathcal{E}_s e^{j\theta_\alpha},\dfrac{\left(\mathcal{E}_s+\sigma_\nu^2\right)^2}{M-\tau}\right) & \mathcal{H}_1.\end{cases} \tag{19}$$

It may be noted that for the signal in addition to the correlated pilots, the cyclic prefix will cause $x[n]$ to exhibit cyclostationarity. As discussed previously these cyclostationary features are weak and are dependent on the length of the cyclic prefix, a function of the channel conditions. In this paper we consider only the effects of pilot induced cyclostationarity. However, the cyclostationarity introduced due to the cyclic prefix may be used to further enhance the performance of the spectrum sensor. It may be observed that under low SNRs, the additive noise forms the dominant component in the estimation error. Also, for wide sense stationary white Gaussian additive noise, the estimation error may easily be shown to be white as in [7]. Therefore, the estimation error components in the finite time cyclic autocorrelation function may be considered as independent for different cyclic frequencies and lags [7]. Thus, the performance of the detector depends on the correct knowledge of the noise variance σ_ν^2, the primary signal energy at the spectrum sensor $\mathcal{E}_s$, and the phase θ_α. However, while the knowledge of σ_ν^2 and θ_α at the spectrum sensor may be assumed, the exact knowledge of $\mathcal{E}_s$ may not be available at the spectrum senor. Nevertheless, as shown subsequently, detectors without the knowledge of these parameters may still be designed but at the cost of detection performance. For a cyclic frequency α the feature vector $\mathbf{r}_\alpha$ may be defined as

$$\begin{aligned}\mathbf{r}_\alpha=&[\Re\{\hat{R}_{yy}^{\alpha}[M,N]e^{-j\theta_\alpha}\},\Re\{\hat{R}_{yy}^{\alpha}[M,2N]e^{-j\theta_\alpha}\},\ldots,\\&\Re\{\hat{R}_{yy}^{\alpha}[M,KN]e^{-j\theta_\alpha}\}]^T\end{aligned} \tag{20}$$

where K is the total number of lags being used as features and $\Re\{.\}$ denotes the real part of a complex number. It is to be noted the variances of different elements of $\mathbf{r}_\alpha$ are different, and therefore optimal linear combiner is the maximal ratio combiner [25]. The vector $\mathbf{w}=[\sqrt{(M-N)},\sqrt{(M-2N)},\ldots,\sqrt{(M-KN)}]^T$, is defined as the

weight vector to combine the cyclostationary features at different lags. Consequently, the test statistic detecting the presence of a signal exhibiting cyclostationarity at a cyclic frequency α may be written as [7,13,26]

$$Z_\alpha = \mathbf{w}^T \mathbf{r}_\alpha = \sum_{k=1}^{K} \sqrt{(M-kN)}\Re\{\hat{R}^\alpha_{yy}[M, kN]e^{-j\theta_\alpha}\}. \tag{21}$$

It may be observed that if the primary user signal exhibits cyclostationarity at more than one cyclic frequency then Z_α for different cyclic frequencies are i.i.d. Gaussian. Let a total of A cyclic frequencies be used for signal detection and $\mathcal{A}$ be the set of the possible cyclic frequencies such that $|\mathcal{A}| = A$. Using all $\alpha \in \mathcal{A}$, the test statistic becomes

$$Z = \sum_{\alpha\in\mathcal{A}} Z_\alpha = \sum_{\alpha\in\mathcal{A}}\sum_{k=1}^{K} \sqrt{(M-kN)}\Re\{\hat{R}^\alpha_{yy}[M, kN]e^{-j\theta_\alpha}\}. \tag{22}$$

From this, it becomes evident that [13]

$$Z \sim \begin{cases} \mathcal{N}\left(0, \dfrac{AK\sigma_\nu^4}{2}\right) & \mathcal{H}_0 \\ \mathcal{N}\left(A\dfrac{N_p}{N_d}\mathcal{E}_s \displaystyle\sum_{k=1}^{K}\sqrt{(M-kN)}, \dfrac{AK(\mathcal{E}_s+\sigma_\nu^2)^2}{2}\right) & \mathcal{H}_1. \end{cases} \tag{23}$$

If the above is used as a test statistic, then the probabilities of false alarm and successful detection for a given threshold λ are given as

$$P_{fa} = Q\left(\frac{\lambda}{\sigma_\nu^2\sqrt{\frac{AK}{2}}}\right) \tag{24}$$

$$P_d(\lambda) = Q\left(\frac{\lambda - A\frac{N_p}{N_d}\mathcal{E}_s\sum_{k=1}^{K}\sqrt{(M-kN)}}{(\mathcal{E}_s+\sigma_\nu^2)\sqrt{\frac{AK}{2}}}\right). \tag{25}$$

It may be observed that the correct knowledge of $\mathcal{E}_s$ is essential for this detector. It is however possible to design a constant false alarm rate (CFAR) detector even in the absence of this knowledge. If σ_ν^2 is unknown at the spectrum sensor, then it may be approximated under low SNRs as [13]

$$\hat{\sigma}_\nu^2 = \frac{1}{M}\sum_{n=0}^{M-1}|y[n]|^2. \tag{26}$$

In case θ_α is not known at the spectrum sensor, then the feature vector may alternatively be given as $\mathbf{r}_\alpha = [\hat{R}^\alpha_{yy}[M, N], \hat{R}^\alpha_{yy}[M, 2N], \ldots, \hat{R}^\alpha_{yy}[M, KN]]^T$ Z_α may be defined as

$$Z_\alpha = \left|\mathbf{w}^H\mathbf{r}_\alpha\right| = \left|\sum_{k=1}^{K}\sqrt{(M-kN)}\hat{R}^\alpha_{yy}[M, kN]\right|. \tag{27}$$

Hence Z_α will be the absolute value of a complex Gaussian random variable. It is well known that for a complex valued random variable $z \sim \mathcal{N}_c(\mu, \sigma)$, its absolute value $r = |z|$ is distributed according to the rice distribution, such that $r \sim \text{Rice}(p, q)$ [27], with the shifting parameter, $p = |\mu|$, and the scaling parameter $q = \frac{\sigma^2}{2}$. Therefore, the distribution of the test statistic under the two hypotheses can be written as,

$$Z_\alpha \sim \begin{cases} Rice\left(0, \sigma_\nu^2\sqrt{\dfrac{K}{2}}\right) & \mathcal{H}_0 \\ Rice\left(\dfrac{N_p}{N_d}\mathcal{E}_s\displaystyle\sum_{k=1}^{K}\sqrt{(M-kN)}, (\mathcal{E}_s+\sigma_\nu^2)\sqrt{\dfrac{K}{2}}\right) & \mathcal{H}_1. \end{cases} \tag{28}$$

Since the cumulative distribution of a non-central Rice distributed random variable cannot be evaluated in closed form, we have to resort to simulation techniques to evaluate the performance of this detector. In this case the detection threshold has to be calculated using the Neyman–Pearson criterion. In a Neyman–Pearson based detector, we fix the maximum allowable false alarm rate and then find a corresponding detection threshold [28]. In this case, to realize a constant false alarm rate spectrum sensor based on the Neyman–Pearson criterion, we generate a large number of independent realizations of the test statistics, and then choose the detection threshold corresponding to the desired probability of false alarm from the sorted realizations of these test statistics.

It is to be noted that the above model though developed for AWGN channels is also applicable to slow fading flat as well as frequency selective channels as described in the section on simulation results. However, as explained in Section 8, the above model is not directly applicable to cases where the channel changes within the sensing duration. An alternative test statistic for the fast fading case has been developed in Section 8.

3. Effects of cyclic frequency offset on a cyclostationarity detector

In the above discussion, it is assumed that the cyclic frequencies of interest are known perfectly at the spectrum sensor. However, this may not always be true. It is observed that the cyclic frequency of a signal may as well be defined as the difference in the frequencies of two correlated components. Therefore, in case the channel introduces a Doppler shift in the signal, the frequencies of the two correlated components will be shifted differently, hence causing an offset in the true cyclic frequency of the signal. Similarly, a sampling clock offset at the spectrum sensor will cause a similar offset in the signal frequencies as described in [14]. It may be noted that most software defined radio systems sample the signal at the intermediate frequency and then digitally down-convert it to baseband. Hence, the effects of Doppler shift and clock offsets will be more pronounced in the baseband as compared to the passband. Therefore, it becomes important to account for these phenomena while detecting a cyclostationary signal. In this section, we study the effects of CFO on the performance of a cyclostationary detector. A practical example for the effects of CFO in sensing an LTE like system follows in the section on simulation results.

For a deterministic signal, $x[n]$, exhibiting second order periodicity, the finite time approximation of the cyclic autocorrelation function may also be written as [18–21]

$$\tilde{R}^\alpha_{xx}[M, \tau] = R^\alpha_{xx}[\tau] * \left(e^{-j\pi\alpha(M-\tau-1)}\frac{sin(\pi(M-\tau)\alpha)}{(M-\tau)sin(\pi\alpha)}\right). \tag{29}$$

where $R^\alpha_{xx}[\tau]$ is the true value of the cyclic autocorrelation function and $*$ denotes convolution over cyclic frequency. If the signal $x[n]$ exhibits cyclostationarity at certain discrete cyclic frequencies whose values are contained in the set Γ, then the cyclic autocorrelation function may be written as

$$\tilde{R}^\alpha_{xx}[M, \tau] = \sum_{\gamma\in\Gamma} R^\gamma_{xx}[\tau]\left(e^{j\pi(\alpha-\gamma)(M-\tau-1)}\frac{\sin(\pi(M-\tau)(\alpha-\gamma))}{(M-\tau)\sin(\pi(\alpha-\gamma))}\right). \tag{30}$$

Now, for $\alpha_m \in \Gamma$, if the cyclic frequency known at the receiver is $\alpha = \alpha_m + \Delta$, where Δ is the CFO introduced due to one or more reasons as described earlier, (30) may be re-written as

$$\begin{aligned}\tilde{R}^\alpha_{xx}[M, \tau] = {} & R^{\alpha_m}_{xx}[\tau]\left(e^{j\pi(\Delta)(M-\tau-1)}\frac{\sin(\pi(M-\tau)(\Delta))}{(M-\tau)\sin(\pi(\Delta))}\right) \\ & + \sum_{\gamma\in\Gamma,\gamma\neq\alpha_m} R^\gamma_{xx}[\tau] \\ & \times \left(e^{j\pi(\alpha-\gamma)(M-\tau-1)}\frac{\sin(\pi(M-\tau)(\alpha-\gamma))}{(M-\tau)\sin(\pi(\alpha-\gamma))}\right).\end{aligned} \tag{31}$$

For small Δ, the second term in (31) may be ignored leading to

$$\tilde{R}^{\alpha}_{xx}[M,\tau] \approx R^{\alpha_m}_{xx}[\tau]g(\Delta, M-\tau) \tag{32}$$

where

$$g(\Delta, M-\tau) = e^{j\pi(\Delta)(M-\tau-1)}\frac{\sin(\pi(M-\tau)(\Delta))}{(M-\tau)\sin(\pi(\Delta))}. \tag{33}$$

It may be observed that, for a fixed Δ, the value of $g(\Delta, M)$ decreases with an increasing M, weakening the features and consequently degrading the detector performance. To avoid this behavior of the detector, Rebeiz et al. in [20] propose to divide the received samples into P non overlapping blocks each of length L ($PL < M$), followed by calculating the finite time approximation of the cyclic autocorrelation function for each of these blocks, and finally averaging these estimates. The feature $\check{R}^{\alpha}_{xx}[P, L, \tau]$ used for detection is thus defined as

$$\check{R}^{\alpha}_{xx}[P,L,\tau] = \frac{1}{P}\sum_{i=0}^{P-1}\frac{1}{L-\tau}\sum_{iL+\tau}^{(i+1)L} x[n]x^*[n-\tau]e^{j2\pi\alpha((n))_L} \tag{34}$$

where $((.))_L$ is the modulo L operator. In this case, a trade-off is required between the values of the block length (L) and the number of blocks (P). It is proposed in [20] to arrive at an optimal combination of L and P using techniques from convex optimization. However, it may be observed that $\tau \leq L$ and hence it is not possible to use the values of the cyclic autocorrelation function at lags greater than the block length as features, thereby limiting the detector performance. This is significant in cases such as the detector proposed in the previous section, where the features exist only for large values of τ. This necessitates to look for alternative methods that avoid the effects of CFO while keeping the number of usable features unaltered. Accordingly, it is proposed that the CFO be first estimated from the available data and then compensated for. Approaches towards improving the performance of adaptive cyclostationary structures by compensating for the CFO have earlier been reported in [18,19,29]. However to the best of our knowledge, no bounds on the performance of a CFO estimator have been reported in the literature so far. Motivated by this, we have discussed the Cramer–Rao bound on the true cyclic frequency estimator in the conference version of this paper [21]. In the following section, we present a detailed derivation of the same.

4. Cramer–Rao bound for the CFO estimator

Assume that M samples of a random cyclostationary signal $x[n]$ containing an additive noise component $\nu[n]$ are received by the spectrum sensor. If $x[n]$ has a cyclostationary component with cyclic frequency α_m with the value of the cyclic autocorrelation function being $R^{\alpha_m}_{xx} = \eta e^{j\phi}$, then for a CFO Δ, the finite time approximate of the cyclic autocorrelation function at a cyclic frequency α and lag τ will be a sum of the noiseless cyclic autocorrelation function with a CFO derived in the previous section and the estimation error due to additive noise. Here again, under low SNR regimes, the estimation error will mainly be due to the additive noise and may safely be assumed as white Gaussian. Substituting (32) in (16), the finite time autocorrelation function for a cyclostationary signal corrupted by noise, and a having CFO Δ, under the alternate hypothesis can be expressed as

$$\hat{R}^{\alpha}_{yy}[M,\tau] = \eta e^{j\phi}g(\Delta, M-\tau) + \zeta[M-\tau] \tag{35}$$

where $\zeta[M-\tau]$ is the error introduced due to a finite averaging effect of the additive noise [13] and $\zeta[M-\tau] \sim \mathcal{N}_c(0, \sigma^2_{\zeta,M-\tau})$ and $\sigma^2_{\zeta,M-\tau} \approx \frac{\sigma^4_{\nu}}{M-\tau}$ for low SNRs. Based on this, the probability density function (pdf) of $\hat{R}^{\alpha}_{xx}[M,\tau]$ may be obtained as

$$p\left(\hat{R}^{\alpha}_{xx}[M,\tau]|\eta,\phi,\Delta\right) = \frac{1}{\pi\sigma_{\zeta,M-\tau}}e^{-\left(\frac{\hat{R}^{\alpha}_{xx}[M,\tau]-\eta e^{j\phi}g(\Delta,M-\tau)}{\sigma_{\zeta,M-\tau}}\right)^2}. \tag{36}$$

Defining

$$\mathbf{r} = \left[\Re\left\{\hat{R}^{\alpha}_{xx}[M,N]e^{-j\phi}\right\}, \Re\left\{\hat{R}^{\alpha}_{xx}[M,2N]e^{-j\phi}\right\}, \ldots, \times \Re\left\{\hat{R}^{\alpha}_{xx}[M,KN]e^{-j\phi}\right\}\right]^T, \tag{37}$$

the pdf of $\mathbf{r}$ may then be obtained as

$$p(\mathbf{r}|\eta\phi\Delta) = \prod_{k=1}^{K}\frac{1}{\sqrt{\pi}\sigma_{\zeta,M-kN}}e^{-\left(\frac{\hat{R}^{\alpha}_{xx}[M,\tau]-\eta e^{j\phi}g(\Delta,M-kN)}{\sigma_{\zeta,M-kN}}\right)^2}. \tag{38}$$

Defining,

$$l(\mathbf{r}|\Delta) = \log(p(\mathbf{r}|\eta,\phi,\Delta)) \tag{39}$$

$$l(\mathbf{r}|\Delta) = \sum_{k=1}^{K}\log\left(\pi\sigma^2_{\zeta,M-kN}\right) - \sum_{k=1}^{K}\left(\frac{\hat{R}^{\alpha}_{xx}[M,\tau]-\eta e^{j\phi}g(\Delta,M-kN)}{\sigma_{\zeta,M-kN}}\right)^2. \tag{40}$$

Defining $f_{x_i}(x_1, x_2, \ldots, x_n)$ as the partial derivative of the function $f(x_1, x_2, \ldots, x_n)$, with respect to x_i

$$l_{\Delta}(\mathbf{r}|\Delta) = 2\Re\left\{\sum_{k=1}^{K}\frac{\eta e^{j\phi}g_{\Delta}(\Delta,M-kN)\left(\hat{R}^{\alpha}_{xx}[M,\tau]-\eta e^{j\phi}g(\Delta,M-kN)\right)}{\sigma^2_{\zeta,M-kN}}\right\}. \tag{41}$$

Since $E[l_{\Delta}(\mathbf{r}|\Delta)] = 0$ therefore, the Cramer–Rao bound on the variance of the estimation error of Δ exists [28].

Therefore, the variance of any arbitrary estimator $\hat{\Delta}$ of Δ must satisfy the following inequality.

$$var\left(\hat{\Delta}\right) \geq \frac{1}{I(\Delta)} \tag{42}$$

where $I(\Delta)$ is the Fisher information about Δ contained in $\mathbf{r}$, defined as $I(\Delta) = -E[l_{\Delta\Delta}(\mathbf{r}|\Delta)]$.

$$l_{\Delta\Delta}(\mathbf{r}|\Delta) = 2\Re\left\{\sum_{k=1}^{K}\frac{\eta e^{j\phi}g_{\Delta\Delta}(\Delta,M-kN)\left(\hat{R}^{\alpha}_{xx}[M,\tau]-\eta e^{j\phi}g(\Delta,M-kN)\right)}{\sigma^2_{\zeta,M-kN}}\right\} - 2\Re\left\{\sum_{k=1}^{K}\frac{\eta^2|g_{\Delta}(\Delta,M-kN)|^2}{\sigma^2_{\zeta,M-kN}}\right\}. \tag{43}$$

As,

$$E\left[\hat{R}^{\alpha}_{xx}[M,\tau]-\eta e^{j\phi}g(\Delta,M-kN)\right] = 0. \tag{44}$$

Hence,

$$E[l_{\Delta\Delta}(\mathbf{r}|\Delta)] = E\left[2\Re\left\{\sum_{k=1}^{K}\frac{\eta^2|g_{\Delta}(\Delta,M-kN)|^2}{\sigma^2_{\zeta,M-kN}}\right\}\right]. \tag{45}$$

Now (Eq. (46) given in Box I.)
For $M - kN \gg 1$

$$|g_{\Delta}(\Delta,M-kN)|^2 \approx \frac{\pi^2}{sin^2(\pi\Delta)}. \tag{47}$$

Substituting this in the definition of $I(\Delta)$ and simplifying

$$I(\Delta) = \frac{2K\eta^2\pi^2}{\sigma^4_{\nu}sin^2(\pi\Delta)}\left[M - \frac{(K+1)N}{2}\right]. \tag{48}$$

$$|g_{\Delta}(\Delta, M-kN)|^2 = \frac{\pi^2}{sin^2(\pi\Delta)}\left[1 - \frac{2\sin(\pi\Delta(M-kN))[\cot(\pi\Delta)\cos((M-kN)\pi\Delta) + \sin((M-kN)\pi\Delta)]}{M-kN} + \frac{sin^2((M-kN)\pi\Delta)csc^2(\pi\Delta)}{(M-kN)^2}\right]. \quad (46)$$

Box I.

Further substituting (48) into (42), the Cramer–Rao bound on the variance of an estimate $\hat{\Delta}$ of Δ may be written as

$$var(\hat{\Delta}) \geq \frac{\sigma_v^4 sin^2(\pi\Delta)}{2\eta^2\pi^2 K\left[M - \frac{(K+1)N}{2}\right]}. \quad (49)$$

It is assumed for the purpose of this derivation that both η and ϕ are known. However, if these parameters are unknown, then the estimator variance will naturally be greater than the case where they are known. This implies that (49) provides the lower bound on the CFO estimator variance for all cases.

Also, an MVU estimator satisfying the CRLB can be determined if there exists a function $h(\mathbf{r})$ of the vector $\mathbf{r}$ such that the first derivative of the log likelihood function satisfies the following condition [28].

$$\frac{dl(\mathbf{r}|\Delta)}{d\Delta} = I(\Delta)(h(\mathbf{r}) - \Delta). \quad (50)$$

However, $l_{\Delta}(\mathbf{r}|\Delta)$ does not contain any polynomial functions of Δ therefore, it is not possible to decompose $l_{\Delta}(\mathbf{r}|\Delta)$ into a form similar to (50). Consequently, the Minimum Variance Unbiased estimator cannot be found directly and becomes necessary to devise alternative estimators for Δ. It may also be observed from (49) that the minimum variance of $\hat{\Delta}$ depends on Δ and that Δ should be minimized in order to minimize the variance of $\hat{\Delta}$. It is evident that $\alpha = \alpha_m + \Delta$, where α_m is the true value of the cyclic frequency and is therefore a constant. Hence, (49) also gives the Cramer–Rao bound for an estimator of the true cyclic frequency of the signal of interest.

If the true cyclic frequency (α) of the SOI is estimated iteratively, then ideally the magnitude of Δ should decrease with each successive estimation thereby reducing the variance of the estimator. Consequently, it is desired to have an iterative estimate of α. The following sections propose two methods which attempt to obtain an iterative estimate of the actual value of the cyclic frequency of the signal of interest from the given samples.

5. The gradient ascent algorithm

It may be seen that the primary signal component of each element r_k of $\mathbf{r}$ is individually maximized when $\alpha = \alpha_m$ and therefore, a linear combination of the same will also be maximized for $\alpha = \alpha_m$. Now, the function $|g(\Delta, M)|$ is concave within the window $\left[\frac{-1}{M}, \frac{1}{M}\right]$, and hence may be maximized by moving along the gradient. Since each element of $\mathbf{r}$ corresponds to $g(\Delta, M)$ with a different M, all of which are maximized at the same point. Maximizing a linear combination of different elements of $\mathbf{r}$ is equivalent to maximizing the individual $g(\Delta, M)$ for each M. Further, if the weights of the different components of $\mathbf{r}$ are assigned in inverse proportion to their variances, then the linear combination of the elements of $\mathbf{r}$ to be maximized is $\mathbf{w}^H\mathbf{r}$. Now, $\mathbf{r}$ can be both real as well as complex, depending on the knowledge of the phase of the cyclic autocorrelation function. Accordingly maximization of the objective function $J = |\mathbf{w}^H\mathbf{r}|^2$ is considered here.

The objective function may be rewritten as

$$J = \mathbf{r}^H\mathbf{W}\mathbf{r} \quad (51)$$

where $\mathbf{W} = \mathbf{w}\mathbf{w}^H$. Differentiating J w.r.t. α

$$\nabla_{\alpha}J = \nabla_{\alpha}\mathbf{r}^H\mathbf{W}\mathbf{r} + \mathbf{r}^H\mathbf{W}\nabla_{\alpha}\mathbf{r} = 2\Re\left\{\nabla_{\alpha}\mathbf{r}^H\mathbf{W}\mathbf{r}\right\}. \quad (52)$$

Considering the more general case where ϕ is not known,

$$r_k = \frac{1}{M-kN}\sum_{n=kN}^{M-1} x[n]x^*[n-kN]e^{-j2\pi\alpha n} \quad (53)$$

and

$$b_k = \nabla_{\alpha}r_k = \frac{1}{M-kN}\sum_{n=kN}^{M-1} x[n]x^*[n-kN]e^{-j2\pi\alpha n}(-j2\pi n). \quad (54)$$

If it is assumed that there is only a small change in $\hat{\alpha}$, the estimate of α, from one iteration to another, then both r_k and b_k can be computed iteratively. These may then be used to update $\hat{\alpha}$, which may again be used to update r_k and b_k. Consequently, the iterative estimation procedure for α based on gradient ascent may be summarized as follows.

1. **Initialize**
   - The number of samples to be used for the initial estimate as B.
   - The cyclic frequency estimate $\hat{\alpha}[B] = \alpha_0$ as the apriori known value of the cyclic frequency.
   - The initial length of feature and the gradient vectors $K = \left\lfloor\frac{B}{N}\right\rfloor$. Based on this, for $1 \leq k \leq K$ initialize the following
   - $r_k[B] = \frac{1}{B-kN}\sum_{n=kN}^{B} x[n]x^*[n-kN]e^{-j2\pi\hat{\alpha}[B]n}$.
   - $b_k[B] = \frac{1}{B-kN}\sum_{n=kN}^{B} x[n]x^*[n-kN]e^{-j2\pi\hat{\alpha}[B]n}(-j2\pi n)$.
   - $w_k[B] = B - kN$.
2. For the nth step, $B < n < M$, update.
   - $K = \left\lfloor\frac{B}{N}\right\rfloor$ Then for $1 \leq k \leq K$ update.
   - $r_k[n] = \frac{n-kN-1}{n-kN}r_k[n-1] + \frac{1}{n-kN}x[n]x^*[n-kN]e^{-j2\pi\hat{\alpha}[n]n}$.
   - $b_k[n] = \frac{n-kN-1}{n-kN}b_k[n-1] + \frac{1}{n-kN}x[n]x^*[n-kN]e^{-j2\pi\hat{\alpha}[n]n}(-j2\pi n)$.
   - $w_k = n - kN$.
3. Based on this, update

$$\hat{\alpha}[n+1] = \hat{\alpha}[n] + 2\mu[n]\Re\{\mathbf{b}^H\mathbf{W}\mathbf{r}\} \quad (55)$$

where

$$\mu[n] = \frac{\mu}{\|\mathbf{b}[n]\|^2}$$

and μ is the step size for adaptation, normalized at each step w.r.t. the instantaneous norm squared value of the gradient. At low SNRs, the contribution of noise to the instantaneous estimates of both the cyclic autocorrelation function as well as gradient will be quiet large and the amplitudes of both will depend mainly on the noise power. This will result in the magnitude of change in each step being dependent on the SNR of the received signal, which is undesirable, therefore, we normalize the step size with the power of the

received signal. The convergence of this algorithm may be proved by following steps similar to those presented in [18].

It is observed that each step requires K^2 complex multiplications. If the value of K is fixed or capped to a maximum then the overall computational complexity of the adaptive algorithm for M samples may be expressed as $\mathcal{O}(MK^2)$.

6. The greedy approach

An alternative approach to find $\hat{\alpha}$ that maximizes the test statistic is to search for it from among all the available cyclic frequencies. As the search for the optimal $\hat{\alpha}$ is being constrained within the main lobe of $g(\Delta, M)$, the size of the search window is inversely proportional to the number of samples being used. Hence, it is preferred to use a smaller number of samples during the search operation so as to keep the optimum $\hat{\alpha}$ within the search window. However, on the other hand, the error introduced due to averaging over a smaller number of samples will be large, thereby reducing the reliability of the estimate. Keeping this in view, an iterative procedure that starts with a large search window but gradually shrinks in size may be a good compromise. It may be a good option here to use a greedy approach which selects $\hat{\alpha}$ that maximizes the value of the objective function within a given search window and then builds the new search window centered around the previous best. Also, since the value of the test statistic will be maximized at the true cyclic frequency, it is a good idea to choose the test statistic as an objective function of the greedy algorithm. Hence, if the value of ϕ is known, then the optimal $\hat{\alpha}$ for a given window will satisfy

$$\hat{\alpha_o} = \arg\max_{\hat{\alpha}} \left\{ \Re \left\{ \sum_{k=1}^{K} (M - kN)(\hat{R}^{\hat{\alpha}}_{yy}[M, kN] e^{-j\phi}) \right\} \right\}. \tag{56}$$

In case ϕ is not known, then the optimal $\hat{\alpha}$ satisfies

$$\hat{\alpha_o} = \arg\max_{\hat{\alpha}} \left\{ \left| \sum_{k=1}^{K} (M - kN)(\hat{R}^{\hat{\alpha}}_{yy}[M, kN]) \right| \right\}. \tag{57}$$

Based on this and following an approach similar to [19], the greedy approach to find the optimum value of $\hat{\alpha}$ may be described as follows.

1. Divide the M received samples into smaller blocks of length L each.
2. **Initialize**
   - The number of sample blocks B to be considered for the initial estimate of $\hat{\alpha}$ so that the initial length of the sample block becomes $Q_B = BL$.
   - The initial estimate of the cyclic frequency, $\beta_B = \alpha$.
   - The iteration counter $q = B$.
3. For $B \leq q \leq \lfloor \frac{M}{L} \rfloor$
   - **Define**
     - The number of lags to be considered for the estimate $k = \left\lfloor \frac{Q_q}{N} \right\rfloor$.
     - The normalized width of the cyclic frequency search window $L_q = \frac{1}{Q_q}$.
   - Split the search window from $\beta_q - L_q$ to $\beta_q + L_q$ into P search points.
   - For each point γ_{qp} around β_q, calculate $\hat{R}^{\gamma_{qp}}_{yy}[qL, kN]$ for $1 \leq k \leq K_q$.
   - Based on the information available about ϕ set the estimate of the true cyclic frequency in the q th stage, β_{q+1} as the cyclic frequency that maximizes (56) or (57).
4. Assign $Q_{q+1} = Q_q + L$ and $q = q + 1$.

The cyclic frequency to be used for sensing is assumed to be the one obtained in the final step of iterations. It may be observed that the calculation of the cyclic autocorrelation function for the q th block with a given lag kN, requires qL complex multiplications and therefore, the search in each window requires $qKLP$ complex multiplications. Now since there are q_{max} such search windows, therefore, the total number of multiplications will become $q_{max}(q_{max} + 1)KLP$ complex multiplications. Since the maximum number of search blocks is, $q_{max} = \lfloor \frac{M}{L} \rfloor$, hence, the number of complex multiplications required is $\left(\lfloor \frac{M}{L} \rfloor^2 + \lfloor \frac{M}{L} \rfloor \right) KLP$. Ignoring the flooring operation, we can write the number of multiplications required as $\frac{M^2}{L} KP + MKP$. Consequently, the overall order of complexity of the proposed algorithm for a fixed K turns out to be $\mathcal{O}(M^2)$.

Table 1
Comparison of computational complexities of different CFO estimation algorithms in terms of complex multiplications.

Algorithm	Complexity
Gradient Ascent	$\mathcal{O}(M)$
Greedy Search	$\mathcal{O}(M^2)$

6.1. Performance of the CFO estimators

The performance of the cyclostationary detector relies on the residual error in the cyclic frequency. It may be observed from the nature of $g(\Delta, M)$ that the spectrum sensing operation will fail if the absolute value of the residual CFO lies above a certain threshold, beyond which the strength of the cyclic autocorrelation function becomes negligible. The 3 dB point in the function $g(\Delta, M)$ may be considered as one such threshold. Therefore, the performance metric for any CFO estimation algorithm may be formulated as a hit/miss function, with the residual CFO lying within the 3 dB window of $g(\Delta, M)$ counted as a hit, and that outside it as a miss. The performance of the CFO estimator may, therefore, be determined in terms of the probability of hit that is the probability of the residual CFO lying within the 3 dB window of $g(\Delta, M)$ for a given number of samples, or the probability of miss which is the probability of the residual CFO lying outside the said window.

Another important factor to consider here is the computational complexity of the CFO estimation algorithm. Ideally, it is desired that the computational complexity of the spectrum sensing algorithm should be linear in the number of samples being used as well as the number of features being employed for detection. However, it is seen that the addition of a CFO estimator to the spectrum sensor results in an additional computational complexity for the spectrum sensor. The computational complexities of the two algorithms considered in our work have been tabulated in Table 1.

7. Simulation results

In this section, simulation results using randomly generated signals are presented. The primary user OFDM signal is assumed to consist of 2048 data subcarriers out of which 256 are pilot subcarriers. A cyclic prefix of length 256 is added to the signal making the total length of the OFDM symbol equal to 2304. It may be observed that for an LTE like system having a sub-carrier spacing of 15 kHz, a 2048 carrier system approximately corresponds to a bandwidth of 30 MHz and an inter pilot spacing of 120 kHz. It is assumed that the passband signal sampled by the spectrum sensor is suitably down-sampled to meet the baseband OFDM signaling rate. It is also assumed that 45 000 signal samples are

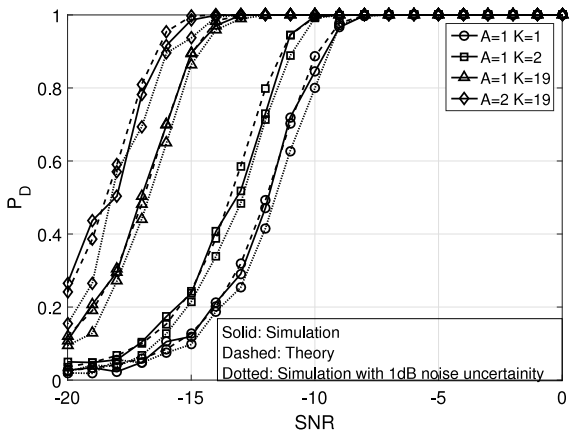

Fig. 1. Performance of the proposed detector for different number of features in the absence of any CFO.

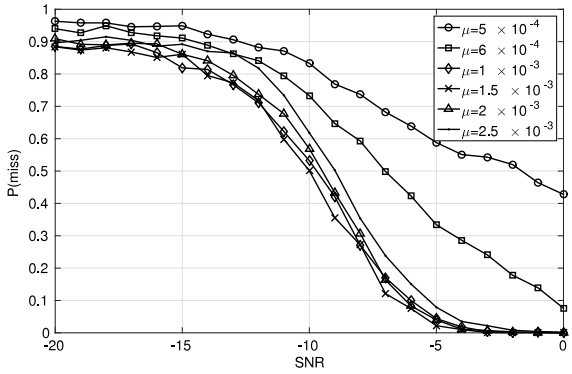

Fig. 2. CFO estimation performance of the gradient ascent algorithm for different step sizes at different SNRs.

used for spectrum sensing. Which for a signaling rate of 30 MHz correspond to a sampling duration of 1.5 ms, and results in $K = 19$ OFDM symbols being used for detection. For the purpose of these experiments, the primary user signal variance is kept constant at unity and the variance of the additive noise is varied to achieve SNRs in the range −20 to 0 dB. Also, it is assumed that the phase of the cyclic autocorrelation function is known at the spectrum sensor. For the experiments involving CFO estimators, the cyclic autocorrelation function at a single cyclic frequency and all the possible lags is considered. It is assumed that the known cyclic frequency is offset by 1% from its true value. This value of the CFO is taken after considering the fact that the effect of Doppler shift in the baseband equivalent of a signal is upper bounded to a few hundred ppm, and the sampling clock offset considered in [14] is of the order of tens of ppm.

The performance of a spectrum sensing algorithm is evaluated in terms of the detection probability at different input SNRs. Unless specified, the detection thresholds are set to give a constant false alarm rate of 1%. Here, 2000 independent trials are conducted to determine the detection performance of the algorithm and 1000 trials are conducted to determine its CFO estimation performance.

7.1. Performance of the proposed detector without any CFO

Fig. 1 illustrates the performance of the proposed detector in the absence of any CFO for different number of lags and cyclic frequencies. It is observed that the simulation results agree with that expected as per the theory derived in Eqs. (24) and (25) . Also,

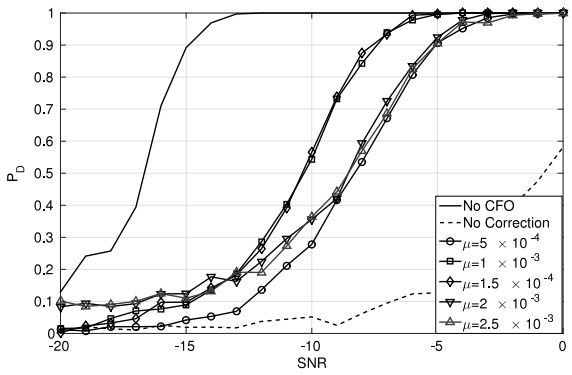

Fig. 3. Detection performance of the gradient ascent algorithm for different step sizes at different SNRs.

it is observed that the derived performance improves considerably as the number of features being used is increased. A gain of nearly 5 dB for a successful detection probability of 90% is observed as the number of features being used is increased from 1 to 19 for a single cyclic frequency. It is also observed that increasing the number of cyclic frequencies from 1 to 2 results in an additional gain of 1.5 dB. This implies that, if for a given number of cyclic frequencies, the number of temporal features are limited then the detector performance will suffer. The effect of uncertainty in noise variance on the proposed spectrum sensor is also studied here. It is observed that the performance of the proposed detector degrades only marginally in the presence of ± 1 dB noise uncertainty, thus showing the robustness of the proposed detector to noise uncertainty.

It may be noted that the detector proposed in [13] uses the conventional autocorrelation at different lags as a feature. This is a special case of our proposed detector for $\alpha = 0$. This case is also plotted in Fig. 1 and is shown to be at par with the proposed detector for a single cyclic frequency.

7.2. Performance of the gradient ascent algorithm in the presence of CFO

Figs. 2 and 3 depict the performance of the gradient ascent algorithm at different SNRs with different step sizes. The number of samples for the initial estimates (B) in these experiments was fixed at 10,000. The estimation error in this case is modeled using a hit/miss function, with a hit corresponding to the final estimate of the cyclic frequency lying within the 3 dB window of true cyclic frequency and a miss corresponding to the final estimate lying outside it. Fig. 2 plots the probability of miss for the gradient ascent algorithm for different step sizes at different SNRs. In both the cases discussed above, the initial CFO is assumed to be 1% of the true cyclic frequency.

It is observed that the performance of the gradient ascent based CFO estimation algorithm is dependent on the step size. Smaller step size means that the system is more likely to ascend the correct gradient. It also results in slower convergence thereby limiting the performance of the estimator as well as the detector. It may be observed from Fig. 2 that a small step size results in a greater probability of miss thereby indicating that the number of samples required by the algorithm for convergence to the true cyclic frequency is larger than the available number of samples. On the other hand, larger step size results in faster convergence of the algorithm but yields a larger residual CFO, again limiting the detector performance. In the present case, it is found via simulation that a step size in the range $(1 - 1.5) \times 10^{-3}$ is a good choice for the given number of samples. The performance loss due to CFO in

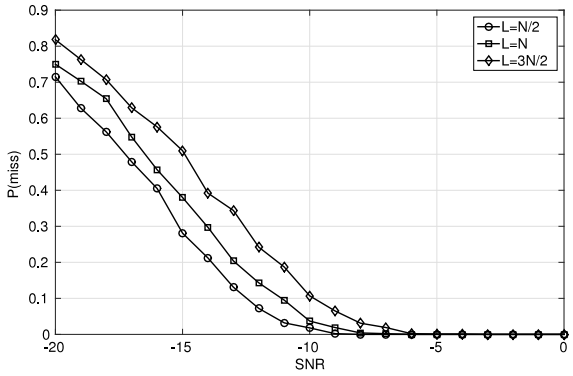

Fig. 4. CFO estimation performance of the greedy search algorithm for different block sizes at different SNRs.

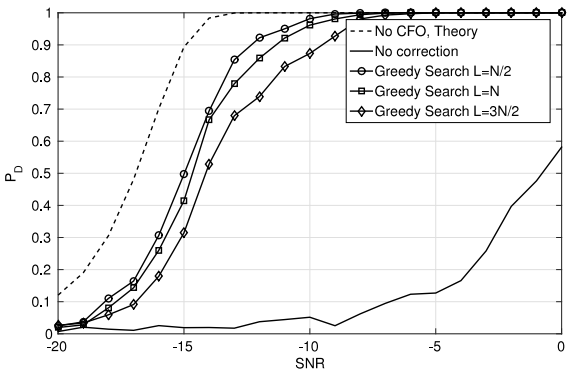

Fig. 5. Detection performance of the greedy search algorithm for different block sizes at different SNRs.

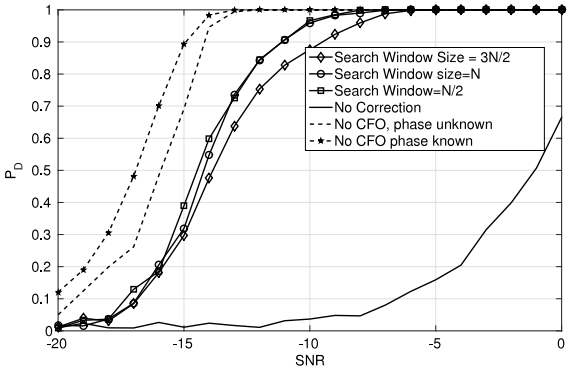

Fig. 6. Detection performance of the greedy search algorithm for different block sizes at different SNRs when the phase of the cyclic autocorrelation function is unknown.

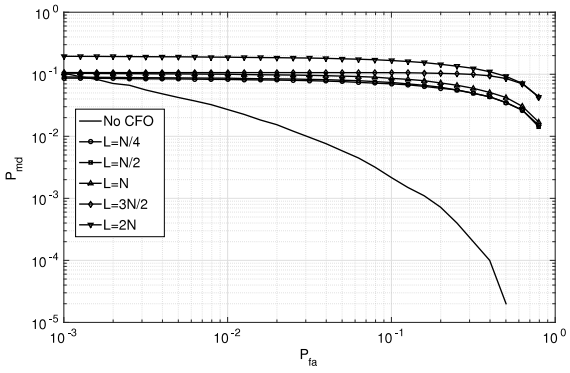

Fig. 7. Complimentary ROCs of spectrum sensor with a greedy search based CFO estimator at an SNR of −10 dB for different block sizes.

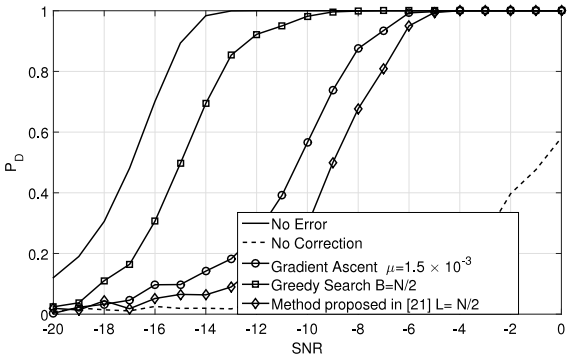

Fig. 8. Detection performance of different CFO compensation schemes at different SNRs.

this case is nearly 7 dB. It may be noted here that smaller step sizes will work better for larger number of samples and vice versa.

Similarly, it is observed in Fig. 3 that the probability of detection performance suffers for both very small and very large step sizes, and the optimal step size lies in the range $(1 - 1.5) \times 10^{-3}$. For a successful detection rate of 60%, a suitable choice of the step size, can compensate for the effects of CFO by as much as 10 dB.

7.3. Performance of the greedy search algorithm in the presence of CFO

In this set of experiments, the variation in the performance of a spectrum sensor with a CFO estimator based on greedy search algorithm for different signal to noise ratios and block sizes is studied. The number of blocks (B) for the initial estimate is given $B = \left\lfloor \frac{10000}{L} \right\rfloor$ for a block size L . Fig. 4 shows the probability of the estimated cyclic frequency lying outside the 3 dB point of the main lobe of the sinc function window centered around the true cyclic frequency for different SNRs. Fig. 5 shows the plots for the probability of detection after the CFO is estimated for an AWGN channel. It may be seen from both these figures that, reducing the size of the search block from $\frac{3N}{2}$ to $\frac{N}{2}$ results in gains of upto 4 dB. However, this improvement in the performance comes at the cost of additional computational complexity.

Fig. 6 plots the detection performance of the spectrum sensor using a greedy search based CFO estimator when the phase of the cyclic autocorrelation function is unknown in different cases. The detection threshold in this case is determined via simulation. 1000 independent trials in the absence of a primary signal are conducted so as to determine the detection threshold for a fixed false alarm rate of 1%. It is observed that the performance in the case of no CFO is slightly degraded in comparison to the case where the phase is known. It is observed that smaller block sizes tend to improve the detection performance by as much as 2 dB for a successful detection rate of 90%. This, however, still shows a loss of more than 2 dB in comparison to the no CFO case.

Fig. 7 shows the complimentary ROCs of spectrum sensor with a greedy search based CFO estimator at an SNR of −10 dB. Also, smaller block sizes result in better detection performances at the spectrum sensor.

7.4. Comparison with the existing method

Fig. 8 compares the performance of different CFO compensation schemes at different SNRs. It is found that the algorithm proposed in [20] performs best for a block size $\frac{N}{2}$ and hence those results may be used as the benchmark for comparison with other methods. It is observed that for a successful detection rate of 90%, the gradient ascent based approach provides a gain of nearly 1 dB while the greedy

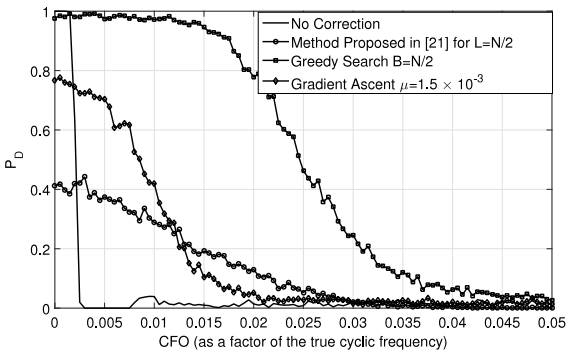

Fig. 9. Detection performance of different CFO compensation algorithms at −10 dB for different values of the CFO.

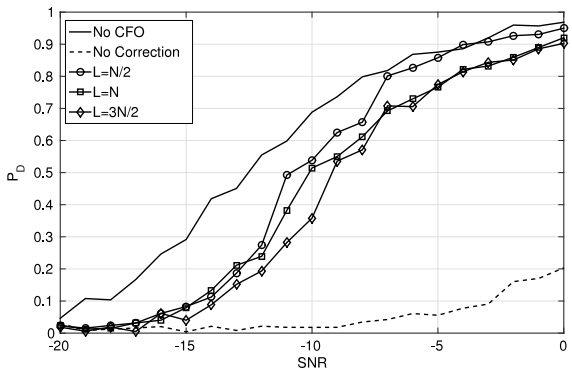

Fig. 10. Detection performance of the greedy search algorithm for different block sizes at different SNRs for a flat fading channel.

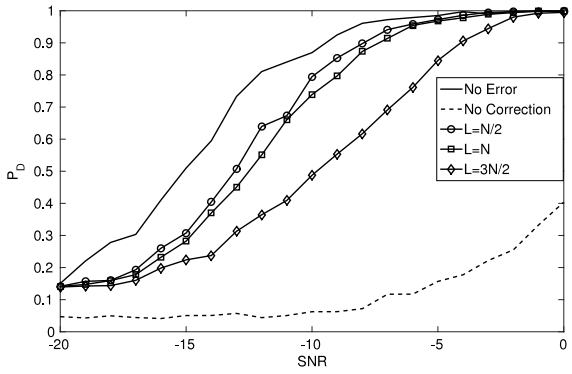

Fig. 11. Detection performance of the greedy search algorithm for different block sizes at different SNRs for a frequency selective fading channel.

search approach results in a gain of nearly 6 dB in comparison to the method proposed in [20].

In Fig. 9, the performances of different CFO compensation methods are plotted against different values of the CFO. It is observed that the gradient ascent algorithm provides good performance for smaller values of the CFO but its performance degrades as the CFO increases. It is also observed that the greedy search algorithm outperforms other methods by a large margin but at the cost of increased computational complexity.

7.5. Performance under fading channels

In the case of a slow fading channel, the received signal under the two hypotheses will be given as

$$y[n] = \begin{cases} \nu[n] & \mathcal{H}_0 \\ \varphi[n] * x[n] + \nu[n] & \mathcal{H}_1 \end{cases} \tag{58}$$

where $\varphi[n]$ is the channel impulse response. This may be represented as a scaler φ for a frequency flat fading channel and a vector $\boldsymbol{\varphi}$, with a length equaling the channel length in the case of a frequency selective channel. In view of this, the distribution of the test statistics under the two hypotheses for a fading channel will take the form [13,30]

$$Z \sim \begin{cases} \mathcal{N}\left(0, \dfrac{AK\sigma_\nu^4}{2}\right) & \mathcal{H}_0 \\ \mathcal{N}\left(\|\boldsymbol{\varphi}\|^2 A \dfrac{N_p}{N_d}\mathcal{E}_s \displaystyle\sum_{k=1}^{K}(M-kN), \dfrac{AK(\|\boldsymbol{\varphi}\|^2\mathcal{E}_s+\sigma_\nu^4)^2}{2}\right) & \mathcal{H}_1. \end{cases} \tag{59}$$

Consequently, the expression for the probability of false alarm remains unchanged as given by (24), but the probability of detection, conditioned on $\boldsymbol{\varphi}$ becomes

$$P_d(\lambda|\boldsymbol{\varphi}) = Q\left(\frac{\lambda - A\frac{N_p}{N_d}\|\boldsymbol{\varphi}\|^2\mathcal{E}_s\sum_{k=1}^{K}\sqrt{(M-kN)}}{(\|\boldsymbol{\varphi}\|^2\mathcal{E}_s+\sigma_\nu^4)\sqrt{\frac{AK}{2}}}\right). \tag{60}$$

The overall probability of detection for a fading channel may be obtained by averaging the above over $\boldsymbol{\varphi}$. This may not be possible analytically and numerical integration may be required, as in [31]. However, detection thresholds for a constant false alarm rate may be obtained by using (24). In this case, the thresholds are determined to keep the false alarm rate fixed at 1%. These thresholds may then be used to determine the corresponding detection rates via simulation. For the purpose of these simulations, the primary signal component in the received signal, when present, is convolved with a channel vector having Rayleigh distributed elements with an exponentially decaying power profile. Following this, the cyclic autocorrelation function of the received signal is calculated for different lags. These are then combined to form the test statistics to be compared against a detection threshold determined by (24). Further, 2000 independent trials were conducted to determine the detection performance. This is done both in the absence and the presence of a 1% CFO. When present, the CFO is corrected by the greedy search algorithm for different block sizes. The performance of the spectrum sensor using a greedy search based CFO estimation for different block sizes under frequency flat fading is compared against the no CFO case and the no correction case as shown in Fig. 10. It may again be observed that for a detection rate of 90%, reducing the search block size from $\frac{3N}{2}$ to $\frac{N}{2}$ results in gains of as much as 4 dB. The performance of a greedy search system under a 128 tap frequency selective fading channel is shown in Fig. 11. It may again be observed that reducing the search block size from $\frac{3N}{2}$ to $\frac{N}{2}$ improves the detection performance by 4 dB.

8. Performance under frequency non-selective fast fading

The Doppler frequency shift, in addition sampling clock offsets is a major reason for CFO. The value of CFO considered in this work is of the order of 1%, that corresponds to a moderately fast fading channel. In this section, we extend the system model presented previously to a fast fading channel, where the channel coherence time is approximately equal to one OFDM symbol duration, and is therefore more than one order of magnitude smaller than the sensing duration. We consider only a frequency non-selective fading channel for the sake of simplicity, however, this model may be extended to a frequency selective channel as well. The signal

received at the nth instant can be written as

$$y[n] = \begin{cases} \nu[n] & \mathcal{H}_0 \\ \varphi[n]x[n] + \nu[n] & \mathcal{H}_1 \end{cases} \tag{61}$$

where, the channel coefficient remains unchanged for each OFDM symbol, and therefore, the channel coefficient for samples contained withing the lth OFDM symbol, i.e. for $n \in \{(l-1)N + 1, \ldots, lN\}$, may be expressed as $\varphi[n] = \varphi^{(l)} \sim \mathcal{N}_c(0, 1)$. Hence, the channels corresponding to K OFDM symbols can expressed as the sequence $\boldsymbol{\varphi} = [\varphi^{(1)}\varphi^{(2)} \ldots \varphi^{(K)}]$. The finite time cyclic autocorrelation function under the alternate hypothesis for a given channel sequence, $\boldsymbol{\varphi}$, can now be written as

$$\begin{aligned} &\hat{R}^{\alpha}_{yy}[M, kN]\,|\mathcal{H}_1, \boldsymbol{\varphi} \\ &= \frac{1}{M-kN}\sum_{n=kN}^{M-1}(\varphi[n]x^{(p)}[n] + \varphi[n]x^{(d)}[n] + \nu[n]) \\ &\quad (\varphi[n-kN]x^{(p)*}[n-kN] + \varphi[n-kN]x^{(d)*}[n-kN] \\ &\quad + \nu^*[n-kN])e^{-j2\pi\alpha n}. \end{aligned} \tag{62}$$

Taking expectation, we can write,

$$\begin{aligned} &E[\hat{R}^{\alpha}_{yy}[M, kN]\,|\mathcal{H}_1, \boldsymbol{\varphi}] \\ &= \frac{1}{M-kN}\Bigg(\sum_{n=kN}^{M}\varphi[n]\varphi^*[n-kN]E\left[x^{(p)}[n]x^{*(p)}[n-kN]e^{-j2\pi\alpha n}\right] \\ &+ \sum_{n=kN}^{M}\varphi[n]\varphi^*[n-kN]E\left[x^{(p)}[n]x^{*(d)}[n-kN]e^{-j2\pi\alpha n}\right] \\ &+ \sum_{n=kN+1}^{M}\varphi[n]E\left[x^{(p)}[n]\nu^*[n-kN]e^{-j2\pi\alpha n}\right] \\ &+ \sum_{n=kN+1}^{M}\varphi[n]\varphi^*[n-kN]E\left[x^{(d)}[n]x^{*(p)}[n-kN]e^{-j2\pi\alpha n}\right] \\ &+ \sum_{n=kN}^{M}\varphi[n]\varphi^*[n-kN]E\left[x^{(d)}[n]x^{*(d)}[n-kN]e^{-j2\pi\alpha n}\right] \\ &+ \sum_{n=kN+1}^{M}\varphi[n]E\left[x^{(d)}[n]\nu^*[n-kN]e^{-j2\pi\alpha n}\right] \\ &+ \sum_{n=kN+1}^{M}\varphi^*[n-kN]E\left[\nu[n]x^{*(p)}[n-kN]e^{-j2\pi\alpha n}\right] \\ &+ \sum_{n=kN+1}^{M}\varphi^*[n-kN]E\left[\nu[n]x^{*(d)}[n-kN]e^{-j2\pi\alpha n}\right] \\ &+ \sum_{n=kN+1}^{M}E\left[\nu[n]\nu^*[n-kN]e^{-j2\pi\alpha n}\right]\Bigg). \end{aligned} \tag{63}$$

Letting $\alpha = \frac{m}{N_d}$ and using the independence of pilots, data and noise along with the fact that only the pilot component exhibits cyclostationary at $\alpha = \frac{mN}{N_d}$ all but the first term of (63) can be eliminated. Therefore,

$$\begin{aligned} E[\hat{R}^{\alpha}_{yy}[M, kN]\,|\mathcal{H}_1, \boldsymbol{\varphi}] &= \frac{1}{M-kN}\sum_{n=kN+1}^{M}\varphi[n]\varphi^*[n-kN] \\ &\quad \times E\left[x^{(p)}[n]x^{*(p)}[n-kN]e^{-j2\pi\alpha n}\right]. \end{aligned} \tag{64}$$

Also, since $x^{(p)}[n] = x^{(p)}[n+kN]$, the above terms can be rearranged as

$$\begin{aligned} E[\hat{R}^{\alpha}_{yy}[M, kN]\,|\mathcal{H}_1, \boldsymbol{\varphi}] &= \frac{1}{M-kN}\sum_{l=k}^{K}\varphi^{(l)}\varphi^{*(l-k)} \\ &\quad \times E\left[\sum_{i=1}^{N}x^{(p)}[i]x^{*(p)}[i]e^{-j2\pi\alpha n}\right] \\ &= \frac{N_p}{N_d}\mathcal{E}_s e^{j\theta_m}\sum_{l=k+1}^{K}\varphi^{(l)}\varphi^{(l-k)}. \end{aligned} \tag{65}$$

The second term is a summation of the products between the channel coefficients for different symbols. This will result in a significantly degraded system performance with the test statistics considered in this work. We therefore need to use different statistics for this case. Assuming symbol level synchronization at the spectrum sensor [14], we can define the test statistic for a sensing duration equivalent K OFDM symbols of length N each, resulting in a total of $M = KN$ samples. We can define the test statistic as

$$\begin{aligned} Z[M, N, kN]\,|\boldsymbol{\varphi} &= \sum_{\alpha\in\mathcal{A}}\sum_{k=0}^{K}\frac{1}{\sqrt{M-kN}}\sum_{l=k+1}^{K}\Bigg|\sum_{i=1}^{N}y[lN+i] \\ &\quad \times\ y^*[(l-k)N+i]e^{-j2\pi\alpha(lN+i)}\Bigg|. \end{aligned} \tag{66}$$

Letting,

$$\begin{aligned} \hat{P}^{\alpha}_{yy}[l, k, N] &= \frac{1}{M-kN}\sum_{i=1}^{N}y[lN+i]y^*[(l-k)N+i] \\ &\quad \times\ e^{-j2\pi\alpha(lN+i)}, \end{aligned} \tag{67}$$

and therefore,

$$\begin{aligned} &\hat{P}^{\alpha}_{yy}[l, k, N]|\boldsymbol{\varphi} \\ &\sim \begin{cases} \mathcal{N}_c\left(0, \dfrac{\sigma_\nu^4}{N}\right) & \mathcal{H}_0 \\ \mathcal{N}_c\left(\varphi^{(l)}\varphi^{*(l-k)}\dfrac{N_p}{N_d}\mathcal{E}_s e^{j\theta_\alpha}, \dfrac{\left(|\varphi^{(l)}\varphi^{(l-k)}|\mathcal{E}_s + \sigma_\nu^2\right)^2}{N}\right) & \mathcal{H}_1. \end{cases} \end{aligned} \tag{68}$$

Consequently,

$$Z[M, N, kN]\,|\boldsymbol{\varphi} = \sum_{\alpha\in\mathcal{A}}\sum_{k=0}^{K}\frac{1}{\sqrt{M-kN}}\sum_{l=k+1}^{K}\left|\hat{P}^{\alpha}_{yy}[l, k, N]\right|. \tag{69}$$

Since $Z[M, N, kN]$ is a summation of absolute values of Gaussian rvs, its exact distribution under the two hypotheses is indeterminable in closed form. However, the performance of this detector can be determined using simulation techniques. Moreover, since the test statistic is not the cyclic autocorrelation function, the characterization of the effects of CFO, and the derivation of cyclic frequency estimators for the same is beyond the scope of this paper. Fig. 12 provides a comparison of the proposed test statistic with the test statistics proposed in the main body of this paper for, AWGN, slow and fast fading channels. For the purpose of this experiment, the channel is assumed to be constant during the sensing duration in case of a slow fading channel, and is assumed to change with each OFDM symbol for a fast fading channel. The fast fading case is realized by multiplying each OFDM symbol with an i.i.d. complex Gaussian fading coefficient, although in practice these coefficients will be correlated for moderately fading channels. It is observed that under slow fading, the test statistic for fast fading channels performs same as the test statistics discussed in the paper. However, for a fast fading channel, the fast fading test

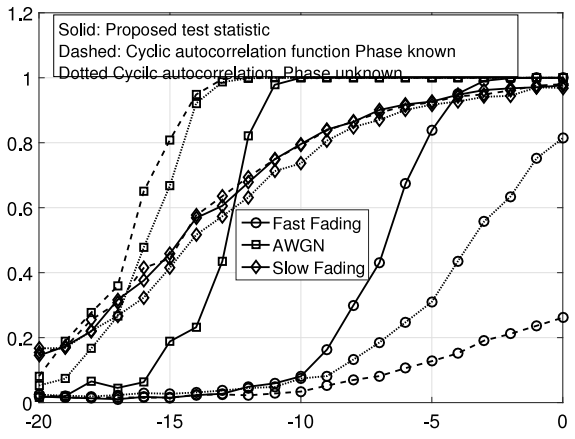

Fig. 12. Detection performance of test statistics for slow and fast fading channels.

statistic results in a 5 dB gain over the test statistics discussed in the paper for a detection rate of 0.8.

It is however to be noted that the above figure compares the performance of the different spectrum sensing schemes under a perfect knowledge of the channel coherence time as well as symbol level synchronization at the receiver, the knowledge of these parameters may not be achievable for spectrum sensing systems. Therefore, it is an important open direction for research to extend this problem to cases without symbol level synchronization at the spectrum sensor.

9. Conclusion

This paper considers the problem of sensing OFDM signals using correlated pilots. It is observed that the inter-pilot correlation causes the OFDM signal to exhibit cyclostationarity which may be used to detect its presence. A feature detector for detecting cyclostationarity at multiple cyclic frequencies and temporal lags is proposed and its performance is derived in case of an AWGN channel. Following this, the effect of any deviation from the known value of the cyclic frequency on the system performance is evaluated. It is observed that for large number of samples, even a small offset in the cyclic frequency may cause severe degradation in the detector performance. The method for compensating the effects of the CFO, as proposed in [20] is studied and is found to be inadequate in case of the proposed detector, where the feature to be detected are placed far apart.

Alternatively, it is proposed to estimate and then compensate for the effects of CFO, thereby enabling the use of all possible features. Derivation of the Cramer–Rao bound on the performance of the CFO estimator, is presented, and it is observed that the variance of the CFO estimator depends on the actual value of the CFO. As a result, it is proposed to estimate the CFO iteratively. Following this, two iterative algorithms are proposed for the purpose. The first is the less complex gradient ascent based algorithm which works only for small values of CFO. The second approach, similar to the one discussed in the conference version of this paper, is based on greedy search which works for larger offsets in the cyclic frequency as well, but at the cost of increased computational complexity. These methods are compared with the algorithm in [20] and it is observed that the greedy search algorithm provides an advantage of more than 6 dB over the method proposed therein but at the cost of computational complexity. Following this, the performance of the proposed detectors under fading channels is studied, and it is found that compensation of CFO leads to gains of as much as 4 dB even under fading channels. It may also be observed that the methods developed in this paper for the purpose of estimation and correction of cyclic frequency offset may be applied to any cyclostationary detector, and may as well be extended to other systems based on cyclostationarity.

However, it is observed that the test statistics used for slow fading are not directly applicable to fast fading channels, therefore developing low complexity fast fading CFO correction algorithms can be a direction for future work.

References

[1] S. Haykin, Cognitive radio: brain-empowered wireless communications, IEEE J. Sel. Areas Commun. 23 (2) (2005) 201–220.
[2] E. Axell, G. Leus, E. Larsson, H. Poor, Spectrum sensing for cognitive radio: State-of-the-art and recent advances, IEEE Signal Process. Mag. 29 (3) (2012) 101–116.
[3] S.M. Kay, Fundamentals of Statistical Signal Processing, Volume II: Detection Theory, Prentice Hall, 1998.
[4] R. Tandra, A. Sahai, SNR walls for signal detection, IEEE J. Sel. Top. Signal Process. 2 (1) (2008) 4–17.
[5] T. Yucek, H. Arslan, A survey of spectrum sensing algorithms for cognitive radio applications, IEEE Commun. Surv. Tutor. 11 (1) (2009) 116–130.
[6] C. Cordeiro, M. Ghosh, D. Cavalcanti, K. Challapali, Spectrum sensing for dynamic spectrum access of TV bands, in: 2ns Intl. Conf. Cognitive Radio Oriented Wireless Networks and Communications, 2007, CrownCom 2007, 2007, pp. 225–233.
[7] A. Dandawate, G. Giannakis, Statistical tests for presence of cyclostationarity, IEEE Trans. Signal Process. 42 (9) (1994) 2355–2369.
[8] S. Chaudhari, V. Koivunen, H. Poor, Autocorrelation-based decentralized sequential detection of ofdm signals in cognitive radios, IEEE Trans. Signal Process. 57 (7) (2009) 2690–2700.
[9] E. Axell, E. Larsson, Optimal and sub-optimal spectrum sensing of ofdm signals in known and unknown noise variance, IEEE J. Sel. Areas Commun. 29 (2) (2011) 290–304.
[10] A. Tani, R. Fantacci, A low-complexity cyclostationary-based spectrum sensing for uwb and wimax coexistence with noise uncertainty, IEEE Trans. Veh. Technol. 59 (6) (2010) 2940–2950.
[11] V. Turunen, M. Kosunen, M. Vaarakangas, J. Ryynanen, Correlation-based detection of ofdm signals in the angular domain, IEEE Trans. Veh. Technol. 61 (3) (2012) 951–958.
[12] H.-S. Chen, W. Gao, D. Daut, Signature based spectrum sensing algorithms for IEEE 802.22 wran, in: IEEE Intl. Conf. Communications, 2007, pp. 6487–6492.
[13] Y. Zeng, Y.-C. Liang, T.-H. Pham, Spectrum sensing for ofdm signals using pilot induced auto-correlations, IEEE J. Sel. Areas Commun. 31 (3) (2013) 353–363.
[14] A. Zahedi-Ghasabeh, A. Tarighat, B. Daneshrad, Spectrum sensing of ofdm waveforms using embedded pilots in the presence of impairments, IEEE Trans. Veh. Technol. 61 (3) (2012) 1208–1221.
[15] Z. Lu, Y. Ma, P. Cheraghi, R. Tafazolli, Novel pilot-assisted spectrum sensing for ofdm systems by exploiting statistical difference between subcarriers, IEEE Trans. Commun. 61 (4) (2013) 1264–1276.
[16] P. Sutton, K. Nolan, L. Doyle, Cyclostationary signatures in practical cognitive radio applications, IEEE J. Sel. Areas Commun. 26 (1) (2008) 13–24.
[17] F.-X. Socheleau, S. Houcke, P. Ciblat, A. Assa-El-Bey, Cognitive ofdm system detection using pilot tones second and third-order cyclostationarity, Signal Process. 91 (2) (2011) 252–268.
[18] J.-H. Lee, Y.-T. Lee, Robust adaptive array beamforming for cyclostationary signals under cycle frequency error, IEEE Trans. Antennas and Propagation 47 (2) (1999) 233–241.
[19] J.-H. Lee, Y.-T. Lee, W.-H. Shih, Efficient robust adaptive beamforming for cyclostationary signals, IEEE Trans. Signal Process. 48 (7) (2000) 1893–1901.
[20] E. Rebeiz, P. Urriza, D. Cabric, Optimizing wideband cyclostationary spectrum sensing under receiver impairments, IEEE Trans. Signal Process. 61 (15) (2013) 3931–3943.
[21] R. Chopra, D. Ghosh, D.K. Mehra, Cyclostationary spectrum sensing for ofdm signals in the presence of ayclic frequency offset, in: 2014 International Conference on Signal Processing and Communications, SPCOM, vol. 1, 2014.
[22] R. Chopra, D. Ghosh, D.K. Mehra, Fresh filter based spectrum sensing in the presence of cyclic frequency offset, IEEE Wirel. Commun. Lett. 5 (2) (2016) 124–127.
[23] H. Ochiai, H. Imai, On the distribution of the peak-to-average power ratio in ofdm signals, IEEE Trans. Commun. 49 (2) (2001) 282–289.
[24] S. Chaudhari, J. Lunden, V. Koivunen, Collaborative autocorrelation-based spectrum sensing of ofdm signals in cognitive radios, in: Information Sciences and Systems, 2008, CISS 2008, 42nd Annual Conference on, 2008, pp. 191–196.

[25] J.G. Proakis, Digital Communication, Mc Graw Hill, 2000.
[26] J. Lunden, V. Koivunen, A. Huttunen, H. Poor, Collaborative cyclostationary spectrum sensing for cognitive radio systems, IEEE Trans. Signal Process. 57 (11) (2009) 4182–4195.
[27] A. Papoulis, Probability, Random Variables and Stochastic Processes, Mc Graw Hill, 2002.
[28] S.M. Kay, Fundamentals of Statistical Signal Processing, Volume I: Estimation Theory, Prentice Hall, 1993.
[29] O. Yeste Ojeda, J. Grajal, Adaptive-FRESH filters for compensation of cycle-frequency errors, IEEE Trans. Signal Process. 58 (1) (2010) 1–10.
[30] W.A. Gardner, Statistical Spectral Analysis A Nonprobabalisitic Theory, Prentice Hall,NJ, 1988.
[31] F. Digham, M.-S. Alouini, M. Simon, On the energy detection of unknown signals over fading channels, in: IEEE Intl. Conf. Communications, 2003, ICC '03, vol. 5, 2003, pp. 3575–3579.

Ribhu Chopra received the B.E. degree in Electronics and Communication Engineering from Panjab University, Chandigarh, India in 2009, and the M.Tech. and Ph.D. Degrees in Electronics and Communication Engineering from the Indian Institute of Technology Roorkee, India in 2011 and 2016 respectively. He is currently an Assistant Professor in the Department of Electronics and Electrical Engineering, Indian Institute of Technology Guwahati. From May 2015 to March 2017, he worked at to the Electrical Communication Engineering department at the Indian Institute of Science under various roles. His research interests include statistical and adaptive signal processing, massive MIMO systems, and cognitive radio communications.

Debashis Ghosh received the B.E. degree in Electronics and Communication Engineering from Malaviya Regional Engineering College, Jaipur, in 1993, and the M.S. and Ph.D. degrees in Electrical Communication Engineering from the Indian Institute of Science, Bangalore, in 1996 and 2000, respectively. He is currently the Professor and Head of the Department at the department of Electronics and Communication Engineering, Indian Institute of Technology Roorkee. From April 1999 to November 1999, he was a DAAD Research Fellow at the University of Kaiserslautern, Germany. In November 1999, he joined the Indian Institute of Technology Guwahati, as an Assistant Professor of Electronics and Communication Engineering. He spent the 2003–2004 academic year as a visiting faculty member in the Department of Electrical and Computer Engineering at the National University of Singapore. Between 2006 and 2008, he was a Senior Lecturer with the Faculty of Engineering and Technology, Multimedia University, Malaysia. His teaching and research interests include communication systems, signal processing, image/video processing, computer vision, and pattern recognition.

D.K. Mehra received the B.E. and M.E. degrees in electrical and communication engineering from the Indian Institute of Science, Bangalore, India in 1968 and 1970 respectively, and the Ph.D. degree from the Indian Institute of Technology, Kanpur, India in 1978. In 1975, he joined the Electronics and Communication Engineering Department of Indian Institute of Technology Roorkee (formerly University of Roorkee) India, where he became a professor in 1987. He was an emeritus fellow from July 2011 to June 2013 in the same department after retirement in June 2011. His main research interests are in the area of adaptive signal processing techniques and their applications in the area of spectrum sensing, interference suppression in CDMA/OFDM systems and digital communication over fading dispersive channels.